Supplementary Material: Quantifying the Consequences of Measles-Induced Immune Modulation for Whooping Cough Epidemiology

Navideh Noori and Pejman Rohani[1-2]

[1]Odum School of Ecology, University of Georgia, Athens, GA 30602 USA

[2]Department of Infectious Diseases, University of Georgia, Athens, GA 30602 USA

February 1, 2019

1 Process Model

We utilized the framework of Partially Observed Markow Process (POMP) [1] to model the interactions between measles and whooping cough mechanistically. Pomp consists of three major components: data, process model and measurement model, as explained in the supplementary material. Here we present the deterministic skeleton of models used for the three different eras. Data from the first two eras were integrated to the same model.

The infection dynamic of whooping cough follows the S, I, R progression, which are susceptible, infectious and recovered classes, respectively. Initially, individuals are susceptible to whooping cough (S). On contracting the disease, they enter the infected class and become infectious (I). Depending on the host age and condition, infection may be fatal. This is presented by *per capita* disease-induced mortality probabilities α_i ($i = 1, 2$), $i = 1$ refers to whooping cough and $i = 2$ refers to measles. The susceptible and infected compartments further sub-divided, S_M and I_M respectively, to take into account individuals who are currently infected with measles. The size of $S_M(t)$ is estimated as weekly mortality cases of measles aggregated over the period of immune suppression (n), corrected for under-reporting, η, as well as disease induced-mortality due to measles, α_2, and considered as a covariate in the model. In equation 1 $i = 0, ..., n$ denotes the number of weeks over which the measles cases are aggregated. $n = 0$ means measles infection affects whooping cough epidemiology within the same week. We chose to fix the measles reporting probability, η, to 52%. In previous studies, the reporting probabilities of measles in England and Wales during the pre-vaccine era were estimated to range from $49 - 55\%$ [2, 3, 4]. Also, based on the literature, disease induced-mortality due to measles, α_2, was fixed to

the values of 0.15 and 0.025 for 1904-1912 and 1922-32 eras, respectively [4]. Therefore, the product values, $\eta \times \alpha_2$, for the first two eras are fixed to 0.078 and 0.013, respectively.

We test whether measles infection increases susceptibility to whooping cough, and we formulate it by a factor θ as susceptibility impact of measles infection. Our first hypothesis implies $\theta > 1$. We also test whether the risk of mortality due to whooping cough is higher after measles infection. Our second hypothesis implies $\alpha^M > \alpha_1$. The equations below describe the deterministic skeleton of transmission model.

$$S_M(t) = \frac{\sum_{i=0}^{n-1} M(t-i)}{\eta \times \alpha_2 N(t)} S(t) \tag{1}$$

$$\frac{dS}{dt} = \nu(t)N(t) - \lambda S_U - \theta\lambda S_M - \mu S \tag{2}$$

$$S_U(t) = S(t) - S_M(t) \tag{3}$$

$$\frac{dI}{dt} = \lambda S_U + \theta\lambda S_M - \gamma I - \mu I \tag{4}$$

$$\frac{dI_M}{dt} = \theta\lambda S_M - \gamma I_M - \mu I_M \tag{5}$$

$$I_U(t) = I(t) - I_M(t) \tag{6}$$

$$R(t) = N(t) - S(t) - I(t) \tag{7}$$

We developed a seasonally forced deterministic continuous-time SIR model. The seasonally forced system in our model is analyzed by making the transmission rate vary sinusoidally which is given in the equations 8 and 9. λ is the force of infection. ι is number of imported cases from outside the population. The mean transmission rate is given by the parameter β, with the amplitude of seasonality b_1 and the peak timing in transmission ϕ. β_0 is the mean transmission rate which is obtained based on the R_0 equation, $R_0 = \frac{\beta_0}{\gamma+\mu}$. μ denotes a constant *per capita* death rate.

$$\lambda(t) = \beta(t)(I_U + I_M + \iota)/N(t) \tag{8}$$

$$\beta(t) = \beta_0(1 + b_1 sin(2\pi(t - \phi))) \tag{9}$$

For the third era (1946-56), we fit the model to the incidence data of measles and whooping cough. Therefore, S_M is estimated as weekly incidence data of measles aggregated over the period of immune suppression, corrected for the under-reporting.

The covariates in our model are the calculated weekly population size, $N(t)$, weekly number of births, $\nu(t) \times N(t)$, aggregated weekly measles mortality data (for 1904-1912 and 1922-32 eras) as well as aggregated weekly measles incidence data (for 1946-56 era), $S_M(t)$. We assume that there is no process noise in our model and the only source of variability in observations is the measurement error. We also developed a model of whooping cough alone with no measles data as a covariate (we call it here SIR) for each era to compare its performance with the model with the interaction term between whooping cough and measles (we call it here SIR-MV) and to test whether addition of interaction terms to the model could help explain the whooping cough data better at the population level. The covariates in the SIR model are $N(t)$ and $\nu(t) \times N(t)$.

2 Measurement Model

Measurement model describes the process by which data are reported and also connects the process model to the data. Mortality cases of whooping cough are assumed to be reported with the probability ratio of ϵ_i. To model the stochastic process of mortality being reported, we assumed that the weekly reported mortality cases are normally distributed. We define $C(t)$ as the total number of fatality cases in week t, of which individuals in $C_1 = \alpha_1 \gamma I_U$ have not experienced any interaction between measles and whooping cough and $C_2 = \alpha^M \gamma I_M$ are individuals infected with whooping cough following measles infection. The normal distribution has the mean of $C(t) = \epsilon_1 C_1 + \epsilon_2 C_2$ and variance of $Var = Var_1 + Var_2$, where $Var_i = \epsilon_i(1 - \epsilon_i)C_i + (\psi_i \epsilon_i C_i)^2$. ψ quantifies overdispersion. The reporting probability of whooping cough, ϵ_i, in England and Wales in different eras were estimated to range from $5 - 25\%$ [5, 6, 7, 8]. We therefore, chose to fix the ϵ_i value to 15%.

For the third era (1946-56), since the incidence data of measles and whooping cough are integrated to the model, α_1 and α^M are excluded from C_1 and C_2 equations, and $C(t)$ is defined as total incidence of whooping cough in week t.

3 Trajectory Matching

We estimated a set of model parameters by fitting the deterministic models to the whooping cough mortality data for the first two eras as well as the whooping cough incidence data for the third era using maximum likelihood (ML) estimation via trajectory matching implemented by Pomp [1]. Since the reporting model is the only source of variability in observations for any fixed set of parameters, we maximized and estimated the likelihood in three steps using Nelder-Mead, Simulated annealing (SANN) and subplex algorithms. Nelder-Mead is a multidimensional unconstrained optimizer without derivatives [9]. SANN is a stochastic global optimization method. It avoids being trapped at local minimums and it can be very useful in getting to a good value on a very rough surface [10]. Nelder-Mead and SANN both use only

function values, are relatively slow and will work for non-differentiable functions. Subplex solves unconstrained optimization problems using a simplex method on subspaces. Subplex is much more efficient than the simplex method and well suited for optimizing noisy objective functions [11]. Estimated parameters include initial conditions, measles-induced immune suppression parameters, disease-induced mortality parameters, transmission related parameters, and observation model parameters.

4 Log-likelihood Profiles

For a dataset Y with k data points in time and model state, x, model predictions are generated using a set of parameters, θ (measurement model). For likelihood-based inference, in the absence of process noise, the likelihood function $L(\theta)$, is a product of conditional likelihood, calculated as the probability of observing each data point at time t given parameters θ; that is, $L(\theta) = P(Y_{1:k}|\theta) = \prod_{i=1}^{k} P(y_t|x_t, \theta)$. We calculate the natural logarithm of the likelihood function, which is the sum of conditional log-likelihood; $\log L(\theta) = \sum_{i=1}^{k} P(y_t|x_t, \theta)$ [12].

We constructed the likelihood profiles for each of measle-induced immune suppression parameters (θ, α^M, n); that is, we varied the value of parameter of interest systematically while maximizing the likelihood over all the remaining model parameters using trajectory matching. Further, a smooth line is fitted through the values at the sampled points. The 95 percent confidence interval is taken to be ~ 2 log-likelihood units below the maximum. To construct two-dimensional log-likelihood surfaces, similar process was done. The two parameters we are inferring; (θ, n), (α^M, n) and (θ, α^M) (Figure S1-S3).

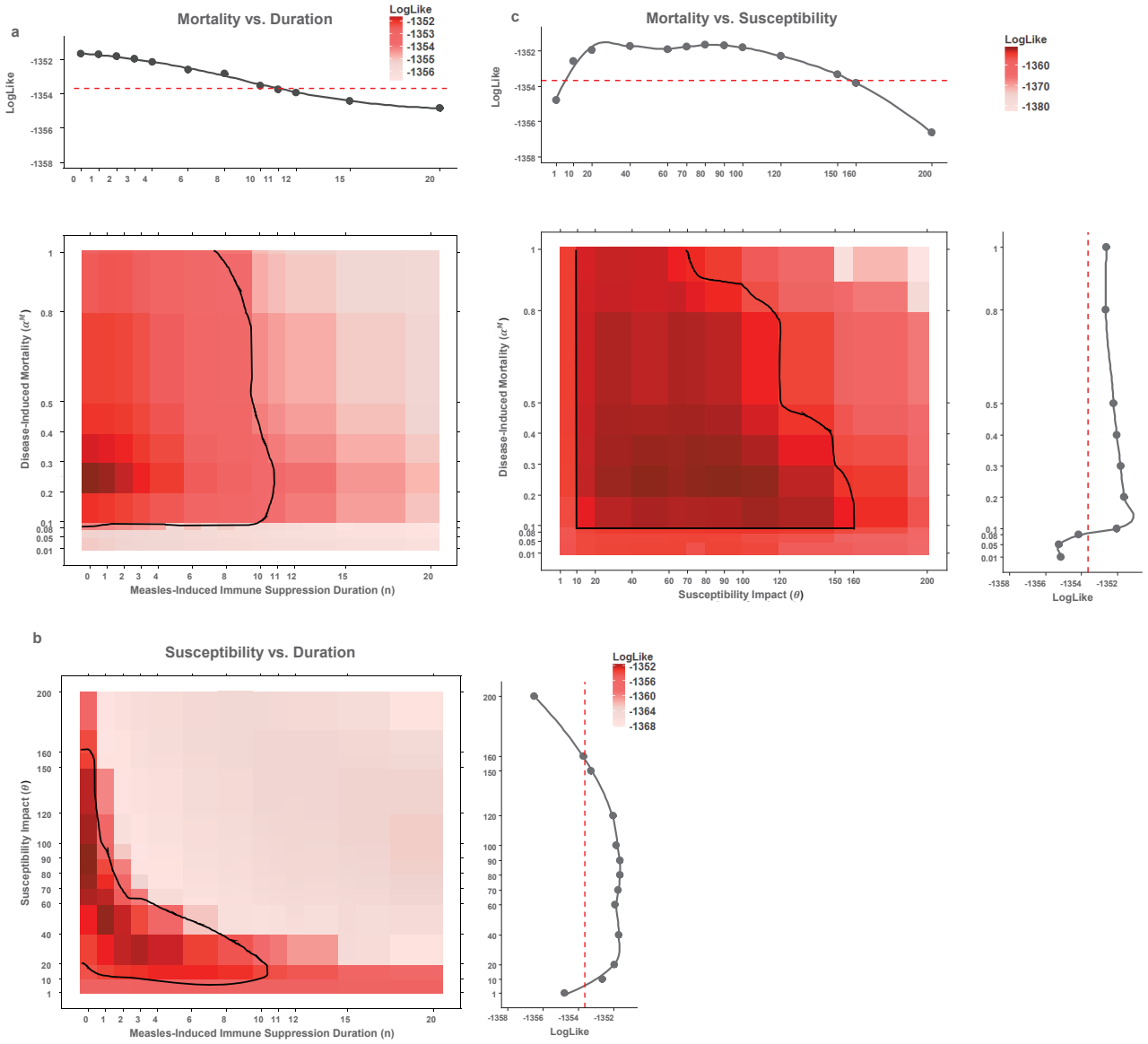

Figure S 1. Two dimensional log-likelihood profiles for parameters (θ, n), (α^M, n) and (θ, α^M) for era 1904-12 in London. The dark red color indicates higher log-likelihood value. The black line in the heat map and the red dashed lines in the side plots represent the the estimated 95% confidence interval.

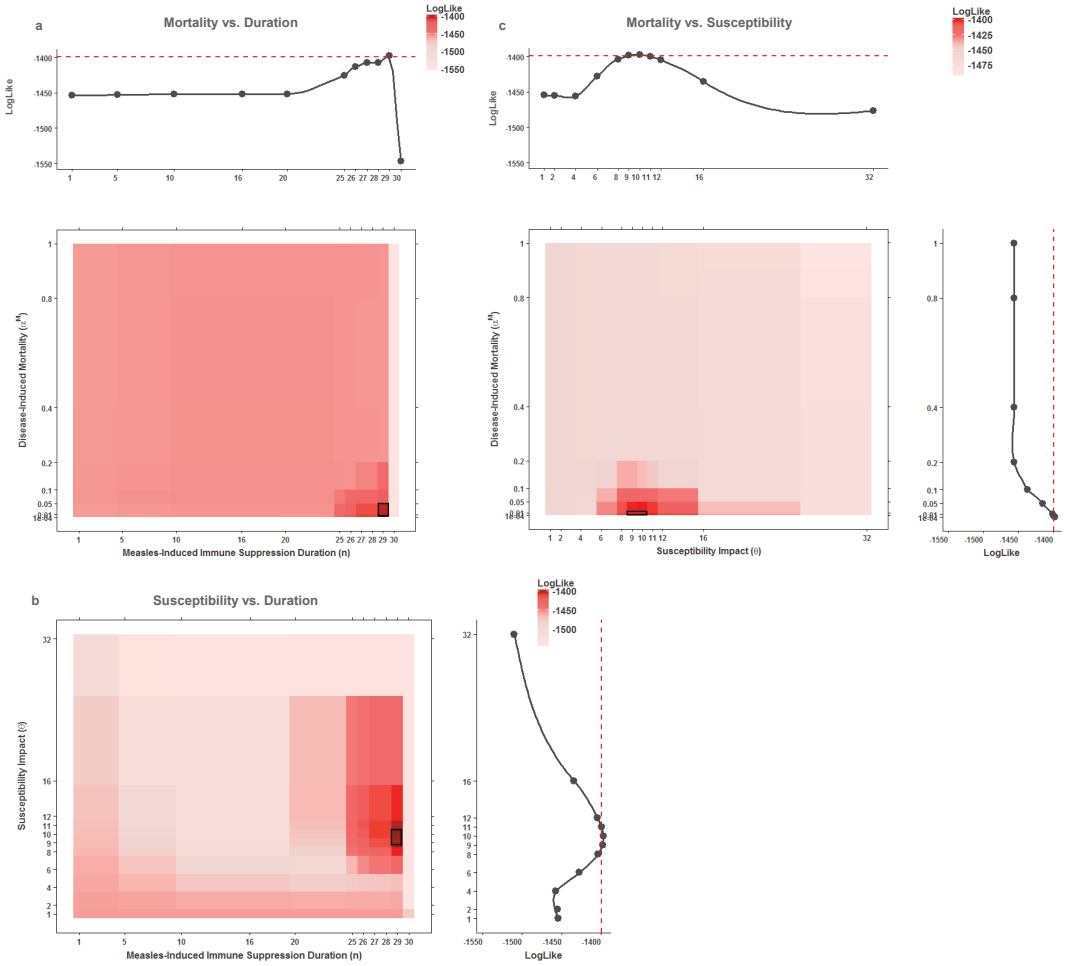

Figure S 2. Two dimensional log-likelihood profiles for parameters (θ, n), (α^M, n) and (θ, α^M) for era 1922-32 in London. The dark red color indicates higher log-likelihood value. The black line in the heat map and the red dashed lines in the side plots represent the the estimated 95% confidence interval.

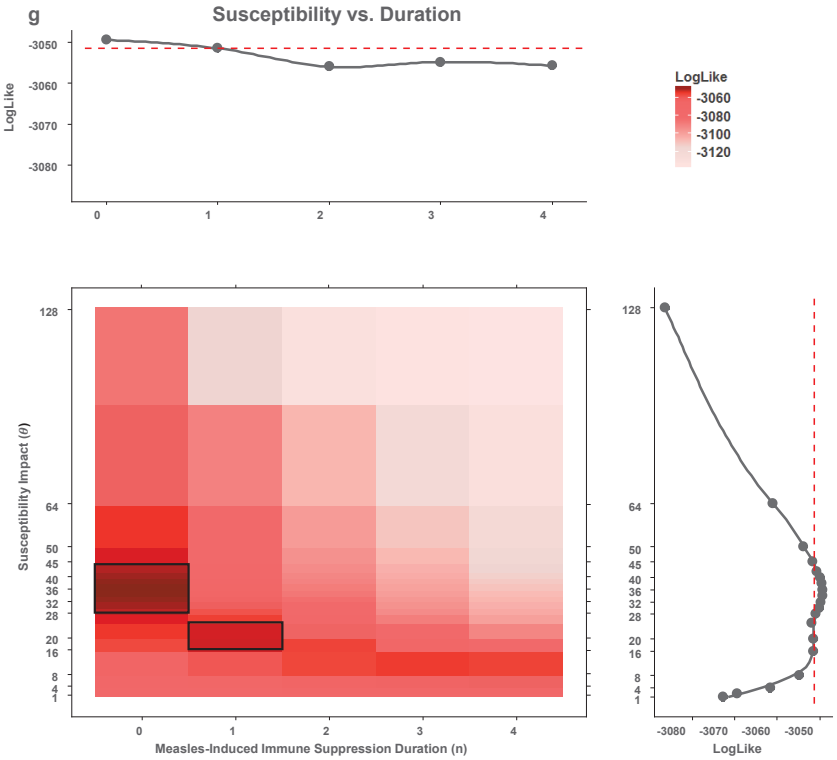

Figure S 3. Two dimensional log-likelihood profile for parameters (θ, n) for era 1946-56 in London. The dark red color indicates higher log-likelihood value. The black line in the heat map and the red dashed lines in the side plots represent the the estimated 95% confidence interval.

5 Models without Interactions

We developed a model of whooping cough alone (SIR) for each era to compare its performance with the model with the interaction term between whooping cough and measles (SIR-MV) and to test whether addition of interaction terms to the model could help explain the whooping cough data better at the population level. To compare the SIR model with the SIR-MV model, Akaike Information Criterion (AIC) was calculated using the following equations.

$$AIC = -2log(Likelihood) + 2H \tag{10}$$

where H is the number of parameters in each model. To compare the model predictions with the data, we simulated the SIR and SIR-MV models 1000 times based on the estimated parameters corresponding to MLE and generated the 95% prediction interval. The results for three eras are given in (Figure S4-S6). The source of fluctuations in the simulated data is the observation noise, and no process noise was considered in our model. Considering that there is no external source of disease reintroduction in the population, $\iota \approx 0$, the simulated time series for the second and third eras, appear to go extinct more frequently than the observed data.

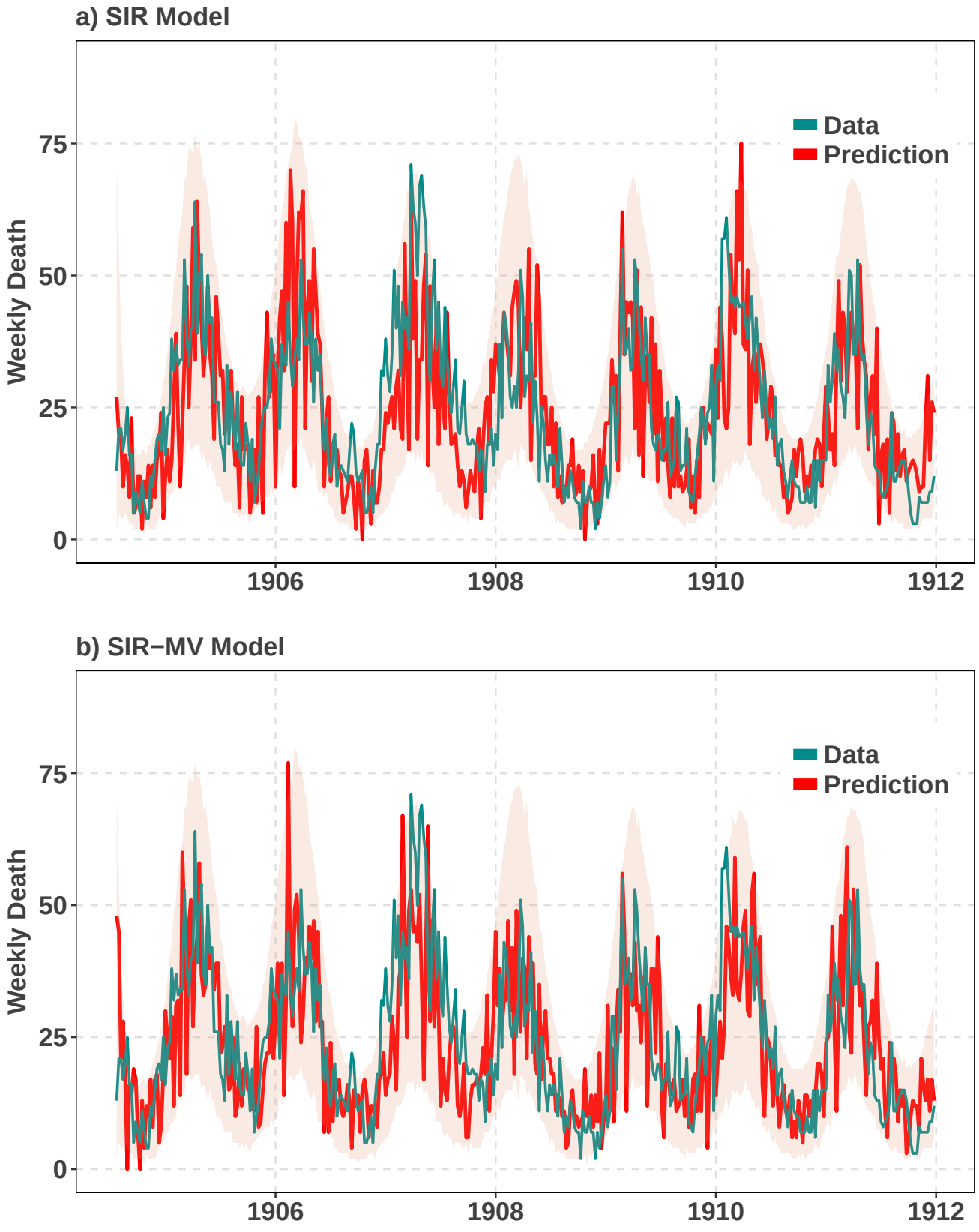

Figure S 4. Weekly notification of whooping cough in London (green line)versus a realization of a) SIR model, b) SIR-MV model (red lines), based on estimated parameters corresponding to MLEs, for the era 1904-12. The highlighted pink area shows the 5 percent prediction interval.

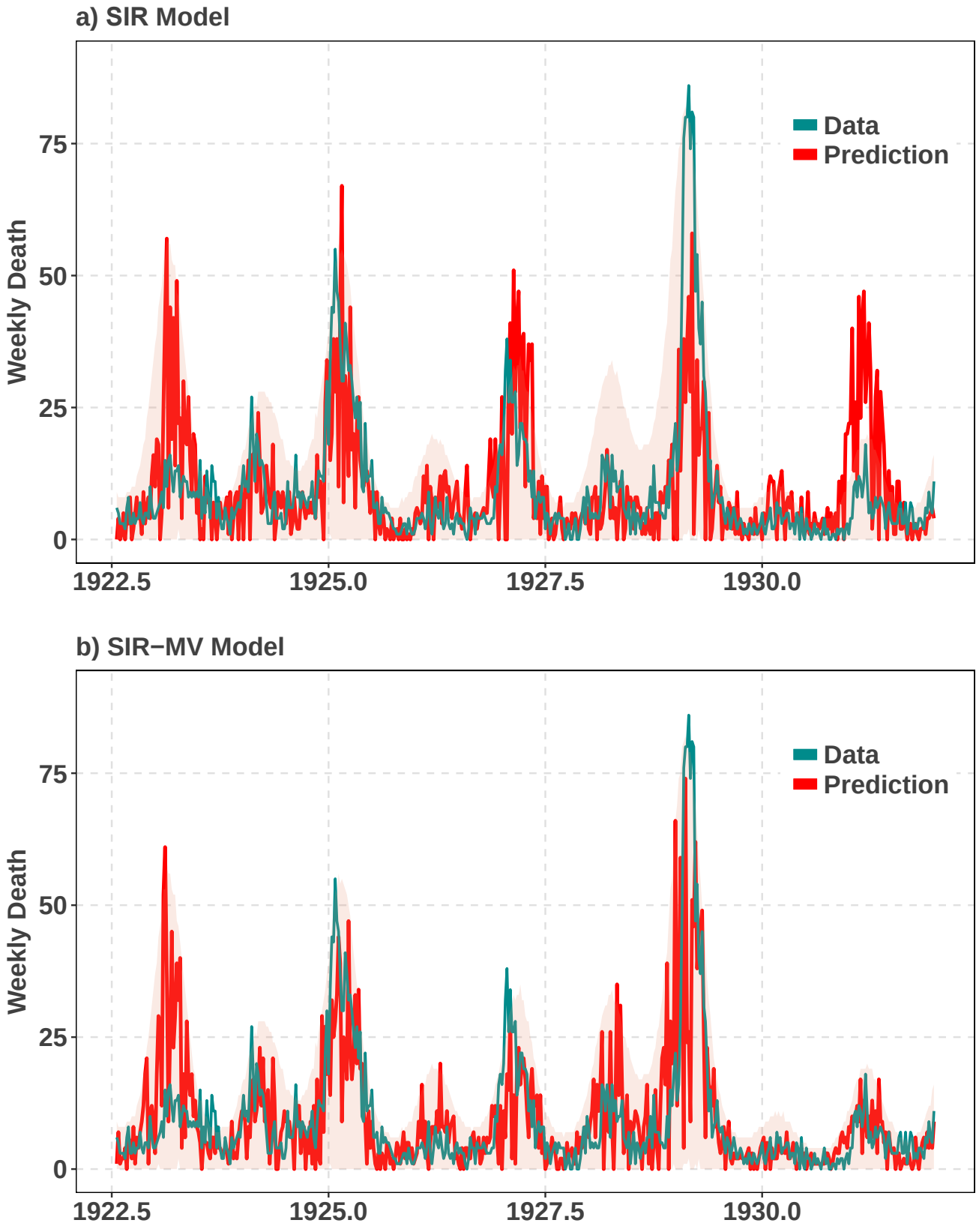

Figure S 5. Weekly notification of whooping cough in London (green line) versus a realization of a) SIR model, b) SIR-MV model (red lines), based on estimated parameters corresponding to MLEs, for the era 1922-32. The highlighted pink area shows the 5 percent prediction interval.

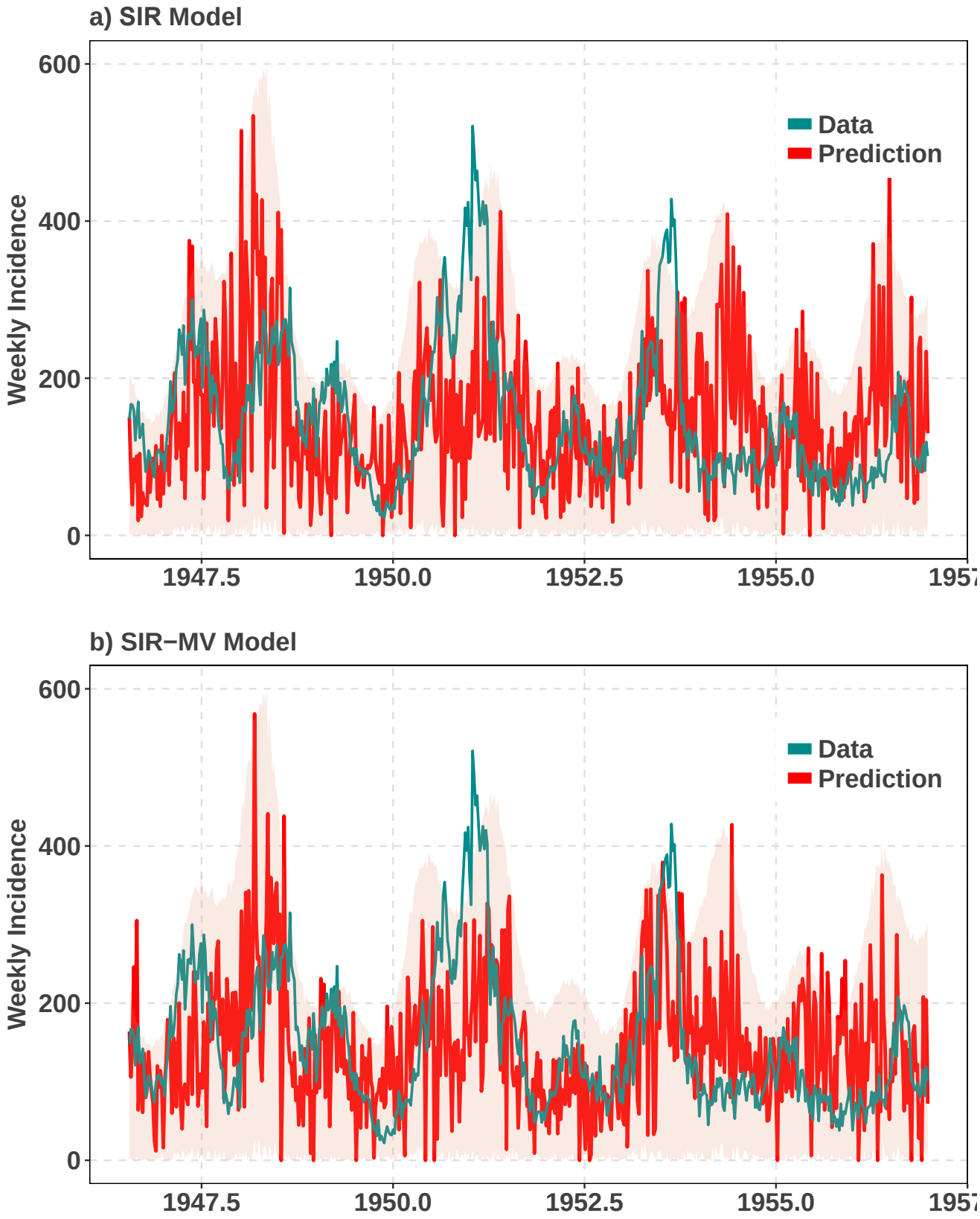

Figure S 6. Weekly notification of whooping cough in London (green line) versus a realization of a) SIR model, b) SIR-MV model (red lines), based on estimated parameters corresponding to MLEs, for the era 1946-56. The highlighted pink area shows the 5 percent prediction interval.

6 Infectious individuals recently infected with measles I_M

We estimated the proportion of individuals in the infectious class who are previously infected with measles (I_M/I) for three eras based on the parameter values corresponding to MLE. Individuals who are recently infected with measles account for 0.1% to 3% of total number of infectious individuals for the first era. The ratio ranges between 0.23% to 19% for the second era, and between 0.023% to 6.5% for the third era (Figure S7).

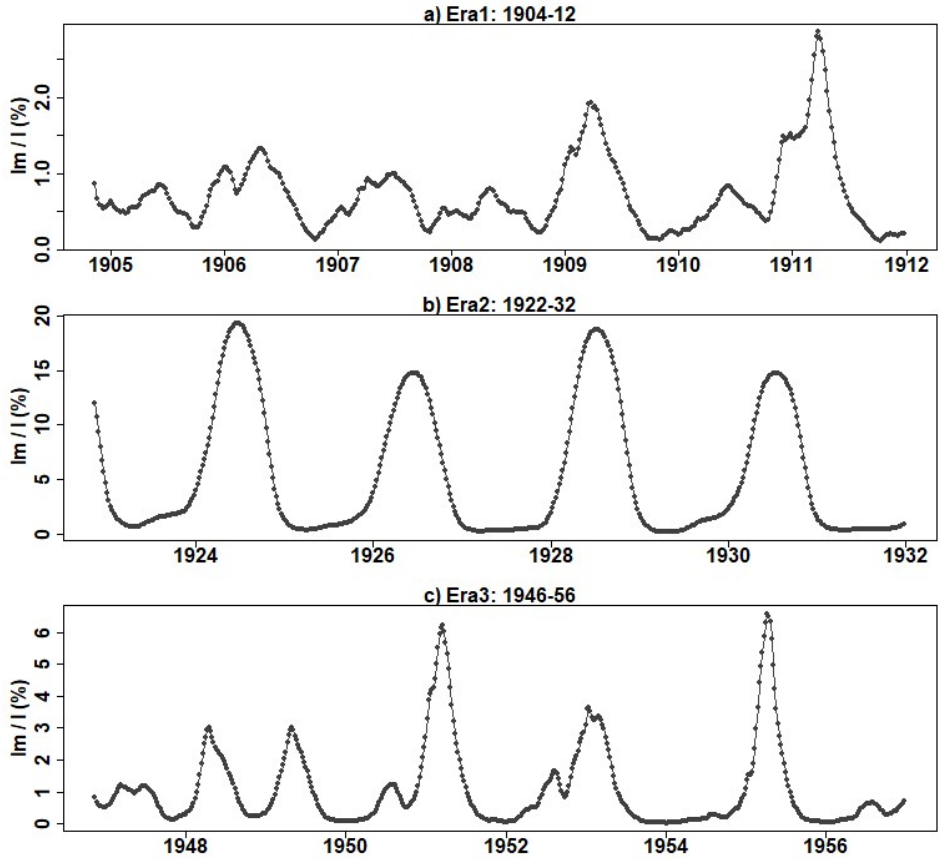

Figure S 7. Proportion of infectious individuals recently infected with measles (I_M/I) for a) era 1: 1904-12, b) era 2: 1922-32, and c) era 3: 1946-46.

7 Sensitivity Analysis

7.1 Fixing R_0 Value For the Era 1922-1932

The estimated R_0 values corresponding to MLE for the era 1922-32, for the SIR model and the SIR-MV model are ~ 29.21 and ~ 8.81, respectively. To make sure that the SIR-MV model is not trapped at a local optima, we forced the model by fixing the value of R_0 to 30 and maximized the likelihood over all

the remaining model parameters. (Table S 1) shows the results. To compare the model prediction with the data, we simulated each model 1000 times and generated the 95 percent prediction interval. The AIC and R^2 values for the model with the $R_0 = 30$ are 2929.47 and 0.26, indicating that the model with the estimated $R_0 = 8.81$ is a better fit to the whooping cough mortality data in this era (Table S 1). Figure S8 shows a realization of SIR-MV model versus the whooping mortality data when R_0 is fixed to 30.

Table S 1. MLE and parameter estimations of SIR-MV model with fixed R_0 for the era 1922-32 in London

Parameters	SIR-MV	SIR-MV with fixed R_0
AIC	2822.24	2929.47
R^2	0.38	0.26
LogLike	-1397.12	-1451.73
R_0	8.81	30 (fixed)
b_1	0.286	0.21
ϕ	0.69	0.71
ι	2.89E-3	0.066
α_1	0.051	0.042
α^M	1.49E-19	0.052
θ	9.77	4.19e-08
n	29	18

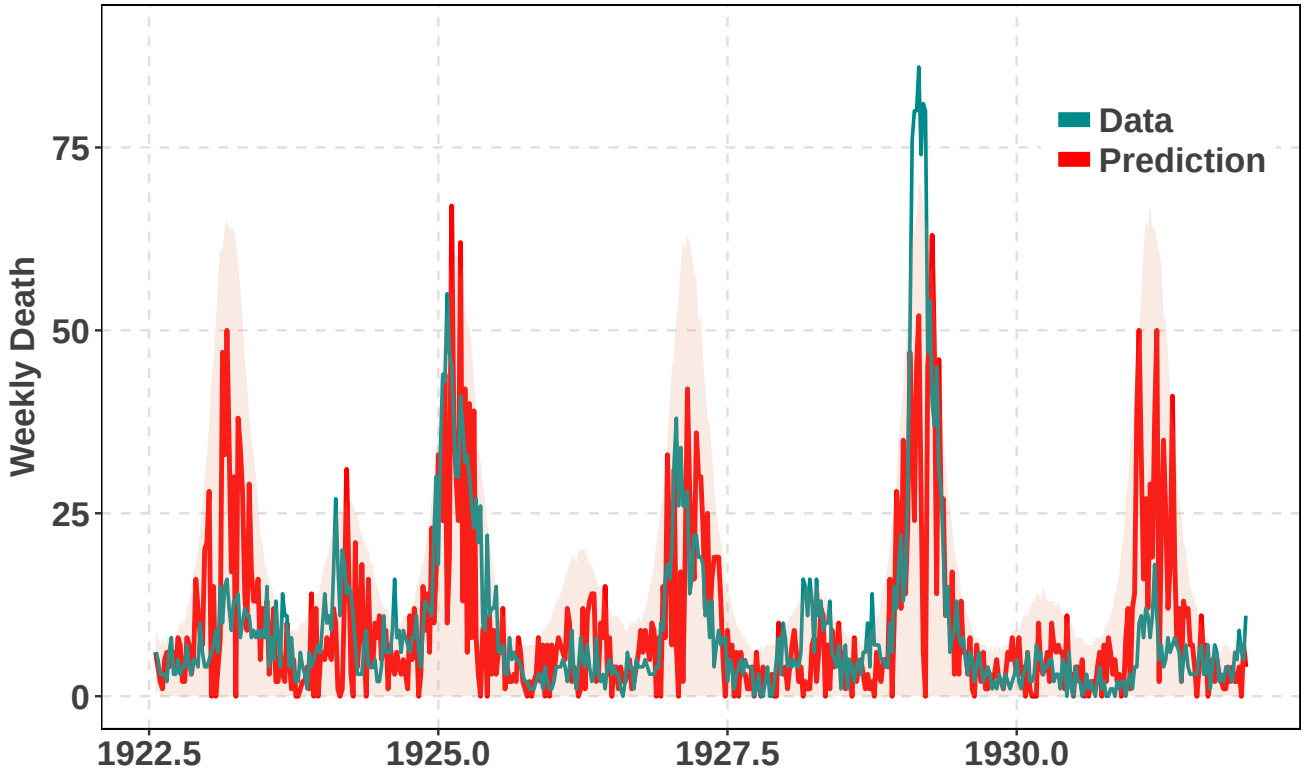

Figure S 8. Weekly notification of whooping cough in London (green line) versus a realization of SIR-MV model with fixed R_0 (red line), based on estimated parameters corresponding to MLEs, for the era 1922-32. The highlighted pink area shows the 95 percent prediction interval.

8 Two-Disease Models

We developed a series of two-disease models that accounted for short-lived measles-induced immune suppression, the effects of measles immune amnesia as well as potential interference effects [13]. These models fitted to the data for all three eras from London. Figure S9 shows schematics of three models. In these models, we assume individuals are born susceptible to both diseases; X_{SS}. Upon recovery from either of diseases, individuals become susceptible to the second disease; X_{RS} and X_{SR}. We test whether individuals become more susceptible and/ore have higher mortality risk due to whooping cough upon recovery from measles, and we formulate them by factors θ and α^M, respectively. In model 2, we examine whether immune amnesia resulting from measles virus infection renders previously infected and recovered individuals susceptible to whooping cough once again. We formulate this hypothesis by a factor of η, which is a proportion of individuals X_{RI} become susceptible to whooping cough again. In model 3, we test whether individuals while infected with measles, X_{SI}, enter a temporary compartment where they become susceptible and infected with whooping cough, X_{ST} and X_{IT}, and whether measles infection increases their susceptibility and risk of mortality due to whooping cough. Individuals after spending some time in the temporary compartment, enter the recovered class, X_{SR}. This period is

formulated by $1/\rho$ which represents the immune-suppression duration.

Table S 2 shows estimated parameter values corresponding to MLEs. Overall, two-disease model 3 performed better than models 1 and 2. SIR-MV model outperformed model 3 with 79, 74 and 39 units smaller AIC, for three eras respectively. Also, from those individuals previously infected and recovered from whooping cough and got infected with measles, none of them are susceptible to whooping cough again (era 1: $\eta = 9.15E-15$, era 2: $\eta = 1.69E-19$, era 3: $\eta = 3.16E-13$).

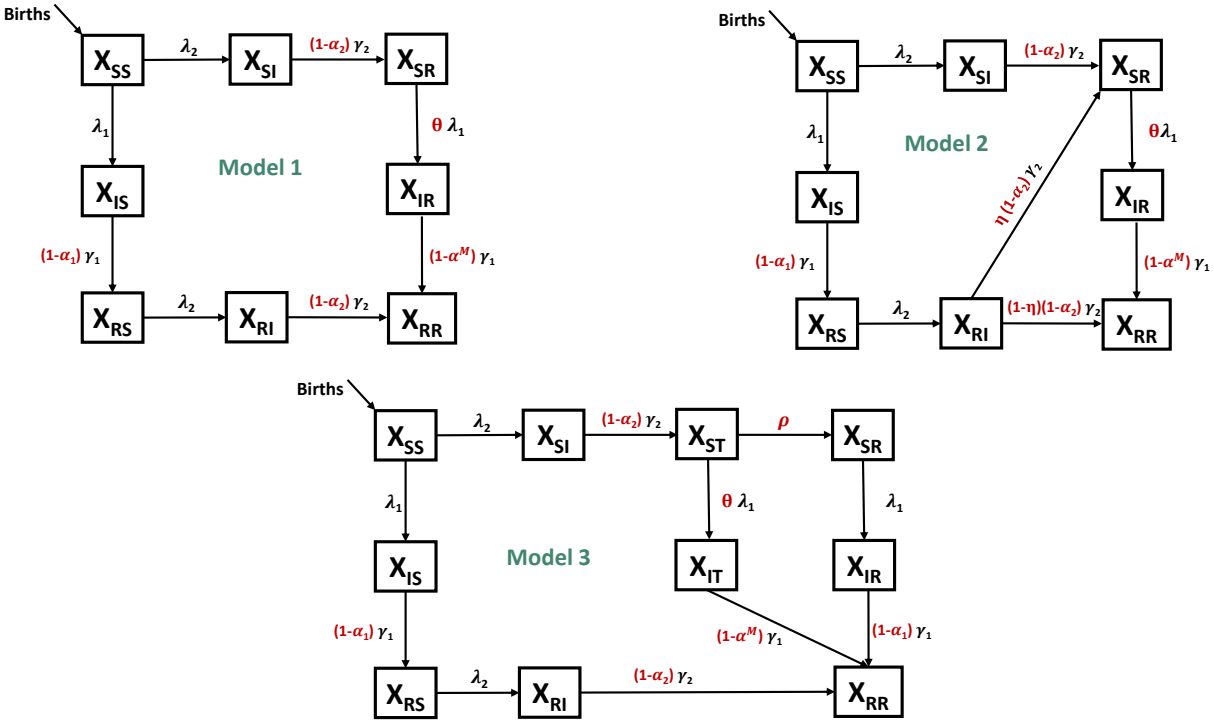

Figure S 9. Schematics of two disease models of measles and whooping cough with various interaction mechanisms. Individuals X_{ij} are categorized based on their status with regards to whooping cough, i, and measles, j.

Table S 2. MLE and parameter estimations of two disease models for three eras. P and M correspond to whooping cough and measles, respectively.

Parameters	Era 1904-12			Era 1922-32			Era 1946-56		
	Model 1	Model 2	Model 3	Model 1	Model 2	Model 3	Model 1	Model 2	Model 3
AIC_P	2829.27	2830.30	2811.72	2912.15	2911.35	2896.307	6242.9	6244.3	6161.99
AIC_M	3069.30	3069.06	3082.32	2458.52	2463.5	2457.3	7069.35	7071.99	7081.44
R_P^2	0.26	0.26	0.12	0.288	0.29	0.31	0.11	0.11	0.167
R_M^2	0.49	0.489	0.18	0.7	0.71	0.72	0.412	0.415	0.4
LogLike-P	-1393.64	-1393.15	-1381.86	-1435.07	-1433.47	-1424.15	-3103.45	-3103.15	-3059.99
LogLike-M	-1513.65	-1512.53	-1517.16	-1208.26	-1209.75	-1204.65	-3516.67	-3516.99	-3519.72
R_{P0}	33.42	32.71	30.8	93.76	89.75	88.34	22.69	22.66	8.57
R_{M0}	29.81	29.82	29.61	57.63	54.71	55.43	35.59	35.57	35.96
b_1	0.12	0.117	0.121	0.147	0.15	0.14	0.17	0.17	0.167
ϕ	3.75	0.76	0.74	0.88	0.87	0.88	0.86	0.88	0.86
ι	0.285	5E-4	2.8E-4	6.92	8.38	8.96	6.87	6.84	6.2
α_1	0.552	0.60	0.55	0.506	0.48	0.49	-	-	-
α^M	0.293	0.3	1	0.166	0.14	2.28E-6	-	-	-
α_2	0.176	0.296	0.128	0.48	0.416	0.38	-	-	-
η	-	9.151e-15	-	-	1.69E-19	-	-	3.16E-13	-
$1/\rho$	-	-	7.8 (days)	-	-	62 (wks)	-	-	401 (wks)
θ	1.35	1.61	4.7	0.5	0.48	0.16	0.68	0.68	0.007
ϵ_P	0.025	0.024	0.021	0.017	0.018	0.016	0.176	0.176	0.086
ϵ_M	0.163	0.099	0.218	0.029	0.032	0.035	0.57	0.57	0.55

9 Simulation study of θ and n

To increase the robustness of our analysis, we carried out a systematic simulation study to examine the identifiability of measles induced immune-suppression duration, n, compared with susceptibility impact parameter, θ. We produced 4 separate simulated time series with combinations of small and large values of n and θ. The selected values of θ are 2 and 100 and the selected values of n are 1 and 25. The values of other parameters in the model were fixed to $R_0 = 29$, $b_1 = 0.16$, $\phi = 0.75$, $iota = 0.006$, $\alpha_1 = 0.075$, $\alpha^M = 0.18$, $\epsilon_i = 0.15$, $\psi_1 = 0.29$,$\psi_2 = 0.41$. We developed two dimensional log-likelihood profile for each combination of n and θ (Figure S10). The results showed that for low values of θ, the immune suppression duration is less identifiable. However, the value of susceptibility impact is identifiable regardless of the value of n.

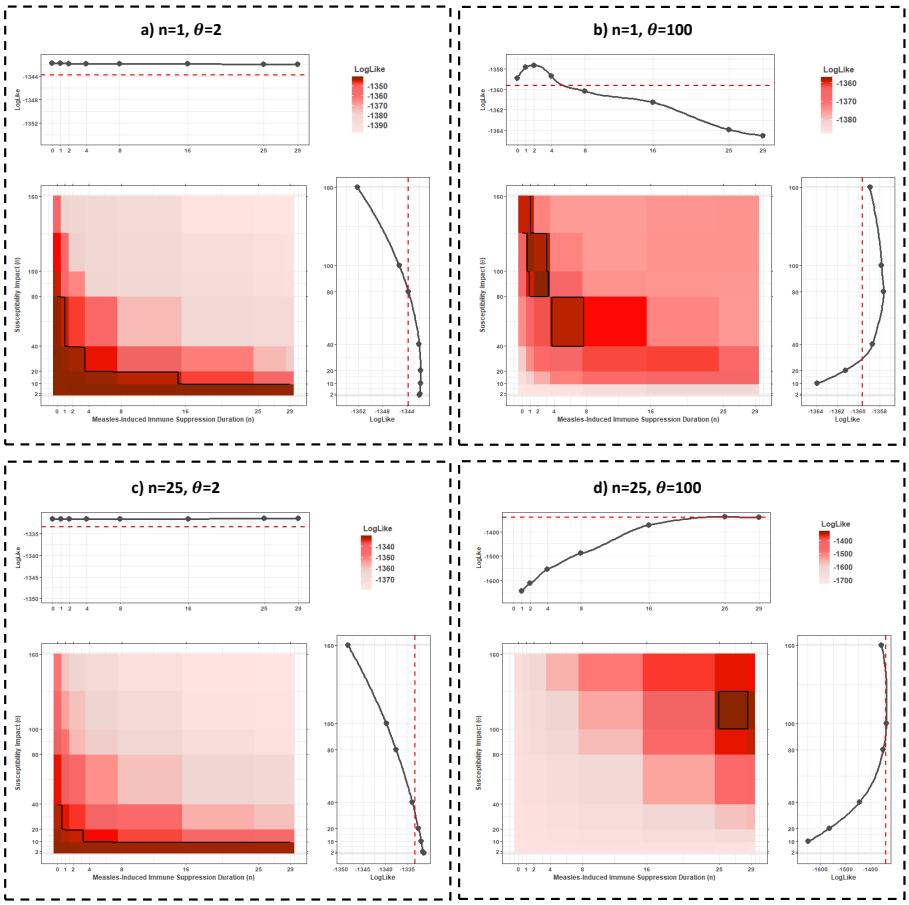

Figure S 10. Two dimensional log-likelihood profile for parameters (n, θ) based on the simulated time series with values of a) (1,2), b) (1,100), c) (25,1), and d) (25, 100). The dark red color indicates higher log-likelihood value. The black line in the heat map and the red dashed lines in the side plots represent the the estimated 95% confidence interval.

10 Simulation study of SIR-MV model

We also carried a separate simulation study to test whether our model can estimate the simulation parameters from aggregate data. We first simulated a time series using SIR-MV model from the first two eras and a set of parameter values as shown in Table S 3. Next, we fitted the simulated data to our model and estimated the parameters. Our fitting algorithm could estimate the parameter values that generated the simulated data correctly.

Table S 3. Parameter values corresponding to simulated data and MLE

Parameters	Simulated Data	MLE
R_0	29.7	29.23
b_1	0.166	0.162
ϕ	0.749	0.746
ι	0.006	0.0227
ψ_1	0.292	0.319
ψ_2	0.417	0.124
α_1	0.075	0.074
α^M	0.18	0.129
θ	70.6	37.53
n	0	1

11 School-term seasonality

To test whether the inconsistencies in our findings could be resolved by using an alternative mechanism of seasonality, we fitted a school-term seasonality to data from London for three eras. The term dates are provided in [14]. Table S 4 shows the estimated parameter values corresponding to MLE. The AIC value is about 90, 330, and 24 units higher than the SIR-MV model with the sinusoidal seasonality, for the three eras respectively.

Table S 4. MLE and parameter estimations of SIR and SIR-MV models using term-time forcing

Parameters	Era 1904-12		Era 1922-32		Era 1946-56	
	SIR	SIR-MV	SIR	SIR-MV	SIR	SIR-MV
AIC	2860.58	2821.12	3305.17	3154.11	6200.38	6146.21
LogLike	-1422.29	-1397.56	-1644.59	-1564.06	-3093.19	-3062.11
R_0	80.39	84.40	135.1	287.8	17.92	20.32
b_1	0.26	0.1	0.516	0.91	0.14	0.11
ι	1.5E-3	8.65E-5	4.91E-6	27.72	2.18E-14	0.027
α_1	0.0739	0.074	0.0439	0.97	-	-
α^M	-	0.082	-	0.018	-	-
θ	-	856.2	-	81970	-	40.59
n	-	0	-	21	-	0

12 Birmingham Data

To test the robustness of our findings, we carried out additional analyses on comparable data from the city of Birmingham (Figure S11). We fitted Birmingham data to SIR and SIR-MV models using maximum likelihood estimation. For the era 1946-46, we also estimated reporting probabilities. To compare the model predictions with the data, we simulated the SIR and SIR-MV models 1000 times based on the estimated parameters corresponding to MLE and generated the 95% prediction interval. The results for three eras are given in Table S 5 and Figure S12-S14. For the first era (1904-12), we found that infection with measles increased susceptibility to whooping cough and also increased the risk of mortality due to whooping cough, however these effects were short-lived. The SIR-MV model did not fit the data any better than a stand-alone SIR model of whooping cough. For the second era (1922-32), there was an increase in susceptibility to whooping cough if an individual had experienced a measles infection within the past six months (Table S 5). Finally, for the data from 1946-56, the estimated duration of the immune modulation effect is 1 week, associated with reduced susceptibility to whooping cough. For the last two eras, forecasts from the best-fitting SIR and the interaction (SIR-MV) models were both in poor agreement with the data.

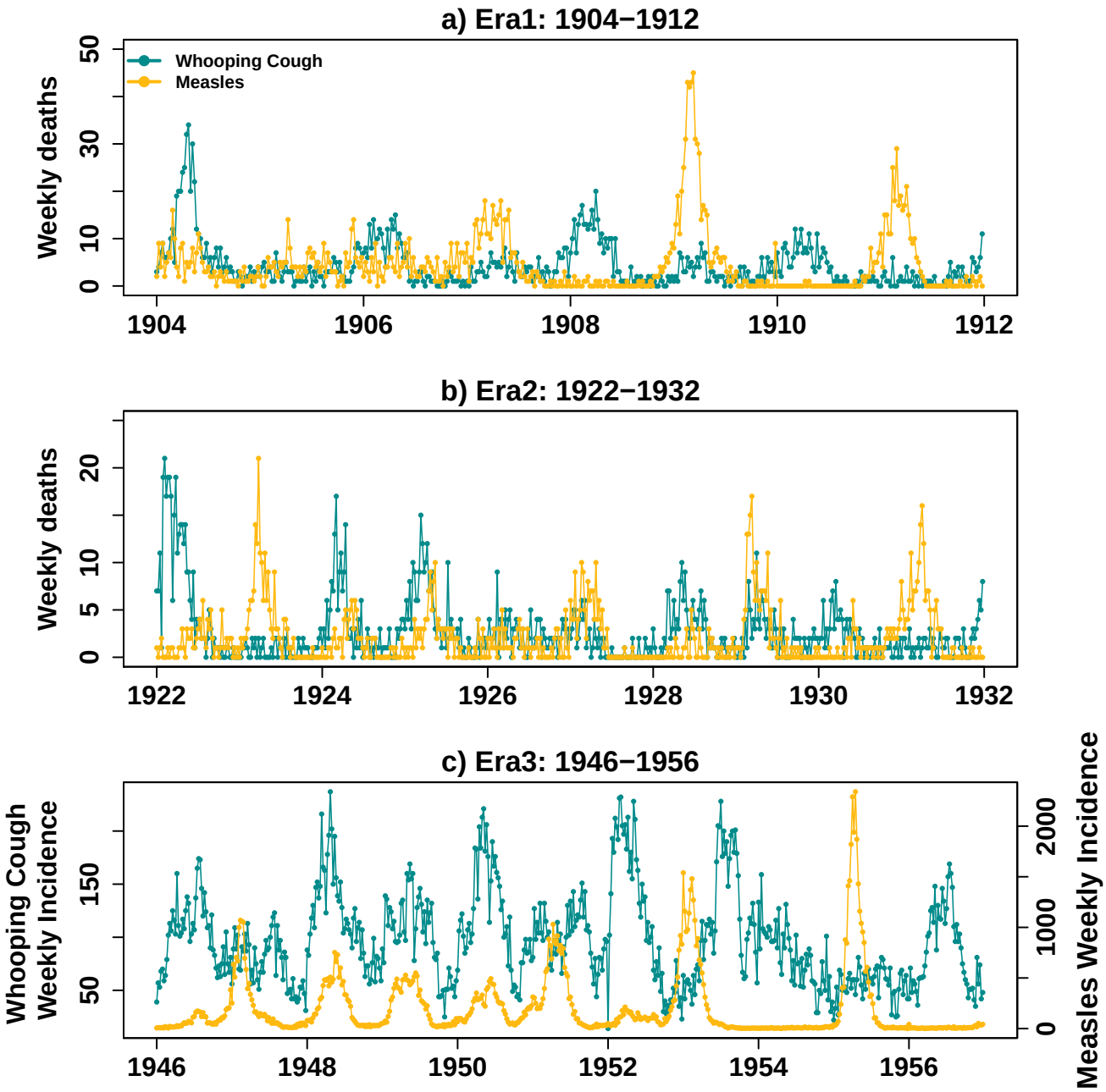

Figure S 11. Weekly notification of whooping cough and measles fatality cases in Birmingham during a) 1904-1912 and b) 1922-1932 and weekly incidence of whooping cough and measles during c) 1946-56.

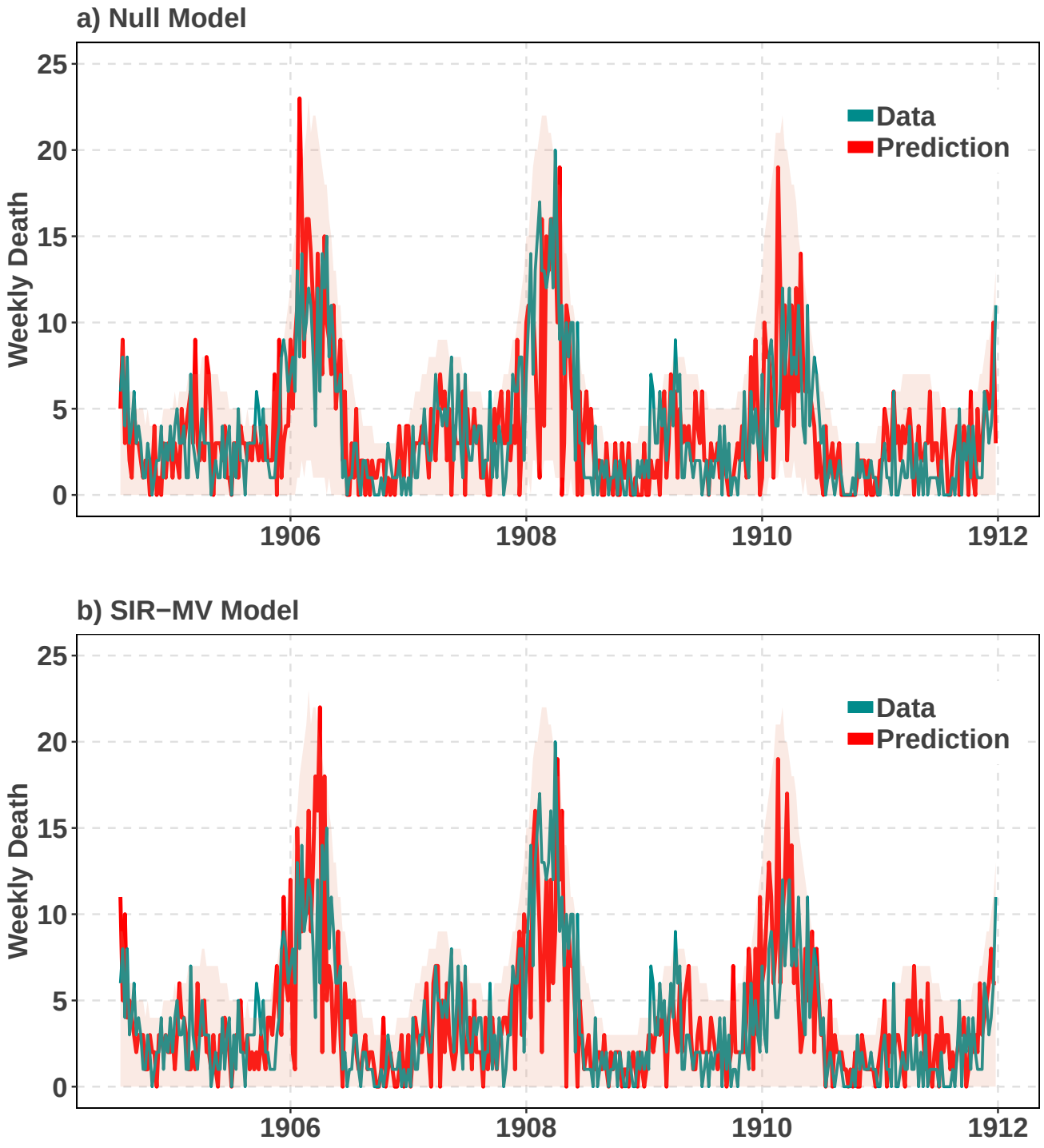

Figure S 12. Weekly notification of whooping cough in Birmingham (green line) versus a realization of a) SIR model, b) SIR-MV model (red lines), based on estimated parameters corresponding to MLEs, for the era 1904-12. The highlighted pink area shows the 5 percent prediction interval.

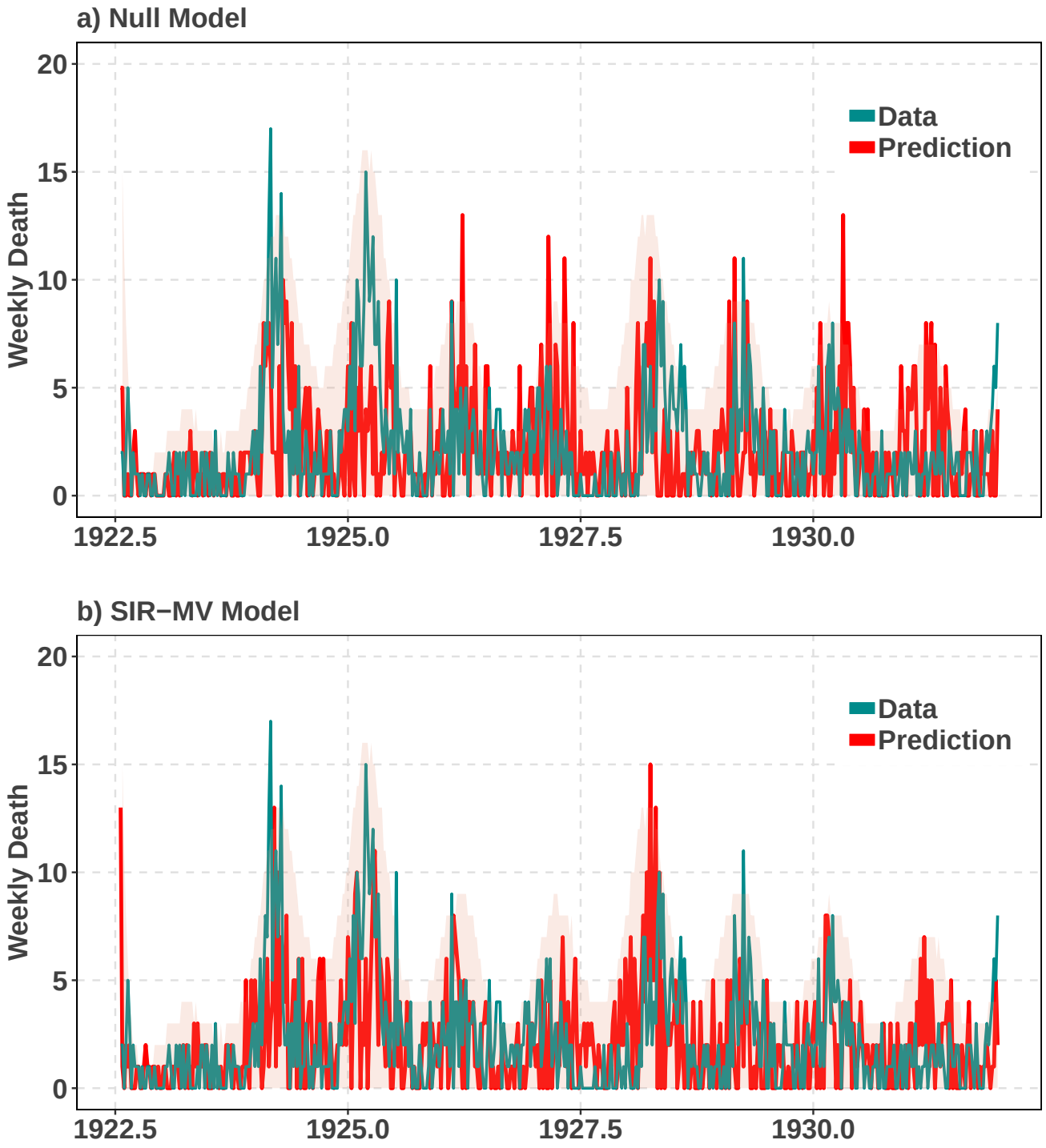

Figure S 13. Weekly notification of whooping cough in Birmingham (green line) versus a realization of a) SIR model, b) SIR-MV model (red lines), based on estimated parameters corresponding to MLEs, for the era 1922-32. The highlighted pink area shows the 5 percent prediction interval.

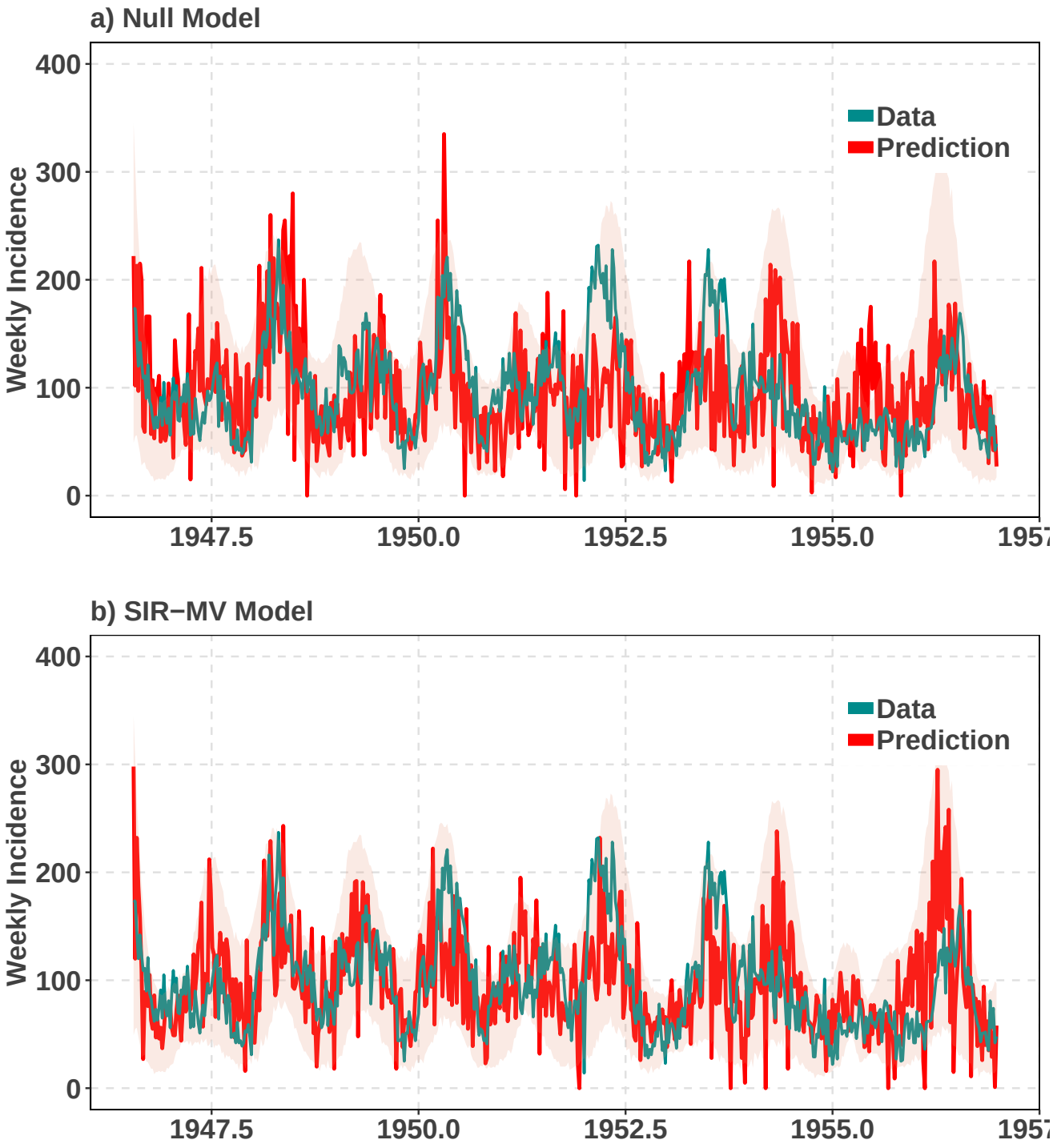

Figure S 14. Weekly notification of whooping cough in Birmingham (green line) versus a realization of a) SIR model, b) SIR-MV model (red lines), based on estimated parameters corresponding to MLEs, for the era 1946-56. The highlighted pink area shows the 5 percent prediction interval.

Table S 5. MLE and parameter estimations of SIR and SIR-MV models using Birmingham data

Parameters	Era 1904-12		Era 1922-32		Era 1946-56	
	SIR	SIR-MV	SIR	SIR-MV	SIR	SIR-MV
AIC	1596.237	1591.97	1858.934	1846.39	5472.16	5310.05
R^2	0.37	0.39	0.07	0.1	0.13	0.2
LogLike	-789.12	-781.98	-920.47	-909.19	-2727.08	-2640.02
R_0	22.73	21.22	23.83	8.86	36.47	29.40
b_1	0.198	0.198	0.21	0.203	0.09	0.189
ϕ	0.75	0.74	0.79	0.73	0.87	0.99
ι	5.98	0.95	81.71	19.48	0.002	410.5
ϵ_1	0.15	0.15	0.15	0.15	0.274	0.246
ϵ_2	0.15	0.15	0.15	0.15		0.703
η	-	-	-	-	-	0.0013
α_1	0.094	0.0907	0.046	0.049	-	-
α^M	-	0.98	-	0.081	-	-
θ	-	37.1	-	4.18	-	0.41
n	-	0	-	29	-	0

References

[1] King AA, Nguyen D, Ionides EL, 2016 Statistical Inference for Partially Observed Markov Processes via the R Package pomp. *J Stat Softw* **69**. doi:10.18637/jss.v069.i12

[2] Finkenstadt BF, Grenfell BT, 2000 Time series modelling of childhood diseases : a dynamical systems approach. *J R Stat Soc Ser C Appl Stat* **49**, 187–205

[3] He D, Ionides EL, King AA, 2010 Plug-and-play inference for disease dynamics: measles in large and small populations as a case study. *J. Royal Soc. Interface* **7**, 271–283. doi:10.1098/rsif.2009.0151

[4] Mantilla-Beniers NB, Bjornstad ON, Grenfell BT, rohani P, 2010 Decreasing stochasticity through enhanced seasonality in measles epidemics. *J. Royal Soc. Interface* **7**, 727–739

[5] Clarkson JA, PE F, 1985 The efficiency of measles and pertussis notification in england and wales. *Int J Epidemiol* **14**, 153–168

[6] Mantilla-Beniers NB, 2004 *Spatio-temporal dynamics of sympatric childhood diseases in the 20 th century*. Ph.D. thesis, University of Cambridge

[7] Lavine JS, King Aa, Andreasen V, Bjørnstad ON, 2013 Immune boosting explains regime-shifts in prevaccine-era pertussis dynamics. *PloS one* **8**. doi:10.1371/journal.pone.0072086

[8] Gunning CE, Ferrari MJ, Erhardt EB, Wearing HJ, 2017 Evidence of cryptic incidence in childhood diseases. *Proc. R. Soc. B* **284**

[9] Nelder JA, R M, 1965 A simplex method for function minimization. *Comput. J* **7**, 308–313

[10] Belisle CJP, 1992 Convergence Theorems for a Class of Simulated Annealing Algorithms on Rd. *J. Appl. Prob.* **29**, 885–895

[11] Rowan TH, 1990 *Functional stability analysis of numerical algorithms*. Ph.D. thesis, University of Texas at Austin

[12] Shrestha S, Foxman B, Weinberger DM, Steiner C, Viboud C, Rohani P, 2013 Identifying the interaction between influenza and pneumococcal pneumonia using incidence data. *Sci. Transl. Med.* **5**, 1–20. doi:10.1126/scitranslmed.3005982

[13] Rohani P, Green C, Mantilla-Beniers N, Grenfell B, 2003 Ecological interference between fatal diseases. *Nature* **422**, 885–888

[14] Keeling RP Matt J, Grenfell BT, 2001 Seasonally forced disease dynamics explored as switching between attractors. *Physica D* **148**, 317–335